Reduction in O-glycome induces differentially glycosylated CD44 to promote stemness and metastasis in pancreatic cancer

Frank Leon[1], **Parthasarathy Seshacharyulu**[1], **Rama K. Nimmakalaya**[1], **Seema Chugh**[1], **Saswati Karmakar**[1], **Palanisamy Nallasamy**[1], **Raghupathy Vengoji**[1], **Satyanarayana Rachagani**[1], **Jesse L. Cox**[2], **Kavita Mallya**[1], **Surinder K. Batra**[1,3,$], **Moorthy P. Ponnusamy**[1,3,$]

[1]Department of Biochemistry and Molecular Biology, University of Nebraska Medical Center, Omaha, NE, U.S.A.

[2]Department of Pathology and Microbiology, College of Medicine, University of Nebraska Medical Center, Omaha, NE, U.S.A

[3]Eppley Institute for Research in Cancer and Allied Diseases and Buffett Cancer Center, University of Nebraska Medical Center, Omaha, NE, U.S.A.

Abstract

Aberrant protein glycosylation has been shown to contribute to aggressive cancer, including pancreatic cancer (PC). Emerging evidence has implicated the involvement of cancer stem cells (CSCs) in PC aggressiveness; however, the contribution of glycosylation on self-renewal properties and maintenance of CSC is understudied. Here, using several in vitro and in vivo models lacking C1GALT1 expression, we identified the role of aberrant O-glycosylation in stemness properties and aggressive PC metastasis. A loss in C1GALT1 was found to result in the truncation of O-glycosylation on several glycoproteins with enrichment of Tn carbohydrate antigen. Mapping of Tn-bearing glycoproteins in C1GALT1 KO cells identified significant Tn enrichment on CSC glycoprotein CD44. Notably, a loss of C1GALT1 in PC cells was found to enhance CSC features (side population-SP, ALDH1+, and tumorspheres) and self-renewal markers NANOG, SOX9, and KLF4. Furthermore, a loss of CD44 in existing C1GALT1 KO cells decreased NANOG expression and CSC features. We determined that O-glycosylation of CD44 activates ERK/NF-kB signaling, which results in increased NANOG expression in PC cells, which facilitated the alteration of CSC features, suggesting that NANOG is essential for PC stemness. Finally, we identified that loss of C1GALT1 expression was found to augment tumorigenic and metastatic potential, while an additional loss of CD44 in these cells reversed the effects. Overall,

$**Correspondence**: Moorthy P. Ponnusamy, Ph.D., and Surinder K. Batra, Department of Biochemistry and Molecular Biology, Eppley Institute for Research in Cancer and Allied Diseases, University of Nebraska Medical Center, Omaha, Nebraska, 68198-5870, U.S.A., Phone: 402-559-1170, Fax: 402-559-6650, mpalanim@unmc.edu and sbatra@unmc.edu.

our results identified that truncation of O-glycans on CD44 increases NANOG activation that mediates increased CSC activation.

Introduction

Cancer is a heterogeneous mixture with a cellular hierarchy wherein self-renewing cancer stem cells (CSCs) constitute a subpopulation of cells distinguishable from the remaining bulk of the tumor. The etiology of cancer is primarily attributed to the self-renewal and maintenance properties of CSC. These cells have the inherent property to divide indefinitely and are unaffected by standard chemotherapeutic regimens, wherein patients succumb to aggressive cancer metastasis [1, 2]. Parallel to stem cells, CSCs are transformed to activate previously inactive self-renewal features and pluripotency by the overexpression of markers, such as SOX, NANOG, KLF4, and OCT3/4 [3]. Although several biochemical techniques have been developed to identify CSCs based on intracellular activity and cell surface expression [4], the regulatory features of tumorigenicity and mechanism of stemness driven by CSC-related genes and glycosylation remain poorly understood.

Glycosylation is a post-translational modification process mediated by resident glycosyltransferases in the Golgi and Endoplasmic Reticulum (ER). Aberrant changes in mucin-type O-glycosylation (herein, referred to as O-glycosylation) have been shown in several malignancies such as breast, prostate, and pancreatic ductal adenocarcinoma (PDAC) [5–9]. The process of O-glycan biosynthesis is initiated by a family of N-acetylgalatosyltransferases (GALNTs) by transferring N-acetylgalactosamine (GalNAc) from uridine 5'-diphosphate-GalNAc (UDP-GalNAc) to serine/threonine (Ser/Thr) amino acid motifs, thus forming the resultant tumor-associated Tn-antigen, GalNAc-O-serine/threonine (Tn-antigen) structure. Next, the extension of Tn-antigens is mediated by core 1 β1,3-galactosyltransferase (C1GALT1), which catalyzes galactose (Gal) transfer from UDP-Gal to GalNAc-O-Ser/Thr, thus forming T-antigens that can subsequently be extended or branched. Recent studies have shown that the expression of tumor-associated antigens due to a loss of C1GALT1, and its folding chaperone, *Cosmc*, are essential for enhancing epithelial to mesenchymal (EMT)-associated genes and the aggressiveness of pancreatic cancer (PC) [7, 10]. However, glycoproteins harboring these aberrantly expressed Tn-antigens to influence CSC maintenance and self-renewal are poorly understood.

In this study, we sought to discover the role of aberrant O-glycosylation on self-renewal properties and the maintenance of CSCs in PC. To identify and characterize cells displaying features of CSCs, we employed the prominent CSC marker, CD44. This marker is widely expressed in cancers and is a single transmembrane non-kinase glycoprotein [11–13]. Several reports implicate glycosylation of CD44 to its function since 20% of the protein sequence harbors putative O-glycosylation sites [13–15]. However, no study has directly addressed the significance and mechanistic implications of aberrant glycosylation of CD44 in the CSC phenotype. We, and others, have previously identified that disruption of C1GALT1 drives the development and enhanced metastatic properties observed in cancer [7, 10]. Using a proteomics approach of enriched Tn-antigen glycoproteins, CD44 was the top candidate identified to harbor Tn-antigens in human PC cell lines engineered for CRISPR/

Cas9 C1GALT1 knockout (KO). Loss of C1GALT1 was shown to alter the O-linked glycosylation of CD44 in human and syngeneic-derived PC cells. Additionally, truncated Tn-antigens on CD44 were found to activate NANOG activation for increased stemness properties through ERK/NF-κB signaling and increased pancreatic tumorigenesis. Our findings begin to contextualize aberrant glycosylation contributions to accelerate metastatic properties by enhanced expression of self-renewal markers and features of pancreatic CSCs.

Materials and Methods

Animals

All animal experiments were performed in compliance with procedures approved by the Institutional Animal Care and Use Committee at the University of Nebraska Medical Center (UNMC).

Cell Lines

Human and murine cell lines were cultured as previously described [7]. Briefly, human PC cell lines (T3M4, HPAF/CD18, SW1990) and syngeneic-derived tumor cells, KPC (Kras$^{G12D/+}$; Trp53$^{R172H/+}$; Pdx-1-Cre) and KPCC (Kras$^{G12D/+}$; Trp53$^{R172H/+}$; C1galt1$^{loxP/loxP}$; Pdx-1-Cre) were cultured in Dulbecco's Modified Eagle Medium (DMEM) containing 10% fetal bovine serum supplemented with 100 μg/ml penicillin-streptomycin at 37°C with 5% CO_2 in a humidified incubator. All human cell lines were negative for mycoplasma contamination and authenticated for short tandem repeat profiling.

Knockout of C1GALT1 to generate human PC cells with truncated O-glycosylation by CRISPR/Cas9

The single guided RNA-CRISPR associated Cas9 system was used to deplete C1GALT1 expression using general cloning protocols [16]. For C1GALT1 KO, a 20 bp target sequence (5'-GCAGATTCTAGCCAACATAA-3') directed against the human C1GALT1 gene was inserted into the guide sequence insertion site of the Cas9-containing CRISPR vector PX330 (42230; Addgene) for transfection of human PC cells using Lipofectamine 2000 (Invitrogen). Following transfection, cells were stained with *Vicia villosa* (VVA) lectin agglutinin fluorescein for fluorescence-activated cell sorting (FACS). Single cells were collected, propagated, and screened for C1GALT1 expressional activity in PC cells using qRT-PCR, immunoblot analyses, and Sanger sequencing.

To generate C1GALT1 KO and CD44 KO clones in human PC cells, a 20 bp target sequence (5'-TCGCTACAGCATCTCTCGGA-3') directed against exon 2 of human CD44 was inserted into PX458 (48138; Addgene) containing-GFP CRISPR plasmid and used to transfect C1GALT1 KO PC cells to generate C1GALT1 KO/CD44 KO cells using JetPRIME (Polyplus Transfection). The cells expressing GFP were subsequently sorted, collected, propagated, and screened by qRT-PCR and immunoblot analyses.

Knockdown of syngeneic-derived cancer cells, KPC and KPCC

Knockdown of *CD44* was performed using shRNA (5'-ATGGCCGCTACAGTATCTC-3') or a control shRNA into pSUPER.retro vector (OligoEngine; VEC-PRT-0002). Plasmids were

packaged into retroviruses using the Phoenix packaging system. Viral supernatants (48hr and 72hr) were collected, filtered, and cultured with syngeneic-derived cancer cells, KPC and KPCC, cell lines at a 1:1 dilution. Transduced target cells were selected with puromycin (Invivogen), and knockdown efficiency was determined by western blot analysis.

Immunoprecipitation and immunoblot analyses

Cell lysates were harvested in chilled RIPA buffer containing complete protease inhibitor (Roche). After centrifugation of 3.0×10^4 RPM for 20 minutes at 4°C, supernatants were collected, protein concentration was measured, and equal amounts of lysates were used for immunoprecipitation per manufactures instructions. Briefly, immunoprecipitation was performed with Dynabeads Protein G (Thermo, 10004D) against CD44 antibody (CST) for 1hr hour at 4°C with shaking and rotation. After that, precipitants were added to magnetic bead-antibody complexes for 30-minute incubation at room temperature under shaking and rotation. The immunocomplexes were washed with PBST three times and eluted with sample buffer for 5 minutes at 70°C. The immunoprecipitated proteins were then separated by SDS-PAGE and transferred to polyvinylidene difluoride membrane (PVDF). For the analysis of glycans by lectin blot analysis, 3% BSA was used for blocking, *Vicia Villosa* (Vector Labs, B-1235) or *Sambucus Niagra* (Vector Labs, B-1305) biotinylated lectin overnight at 4°C, and streptavidin-horse radish peroxidase (HRP) was applied to visualize bands using chemiluminescence reagents (Thermo). For immunoblot analysis, specific antibodies and secondary HRP-conjugated anti-mouse or anti-rabbit antibodies were used. Detailed antibody information is listed in Supplementary Table 1.

VVA enrichment

To enrich Tn-antigens, a total of 1mg of lysate was mixed with 50 μl of biotinylated VVA lectin, and the volume was made up to a total of 1 mL containing PBS. The mixture was added to shaking and rotation overnight at 4°C. The next day, 60 μl of a 1:1 suspension of agarose-coupled streptavidin was added and incubated for an additional four hours. Following incubation at 4°C, the agarose-bound VVA enrichment was washed five times with PBST and subsequently eluted with a 2X sample buffer at 95°C for 5 minutes. The samples were separated by 10% SDS-PAGE gel and subjected to immunoblotting.

In-gel digestion

SDS-PAGE separated eluted glycoproteins, and gels were stained with InstantBlue one-step gel stain (Midsci) for 30 min. The gel pieces were incised after they were briefly washed with HPLC water and then dehydrated with acetonitrile (ACN). Proteins were reduced with 2 mM Tris(2-carboxyethyl)phosphine (TCEP) in 50 mM ammonium bicarbonate (AmBic) for 1 h at 37 °C, and dehydrated with ACN. The reduced proteins were alkylated with 50 mM iodoacetamide (IAA) in 50 mM AmBic for 30 min in the dark with rotation and dehydrated with ACN. MS-grade trypsin (Promega) was added, and gels were incubated on ice for 30 min. Subsequently, 25 mM AmBic was added to cover the gel pieces, and protein digestion was continued overnight at 37 °C. Digested peptides were extracted from the gel with 50% ANC/0.1% trifluoroacetic acid solution, dried in a SpeedVac, re-dissolved in 0.1% formic acid (FA), and submitted for LC-MS/MS analysis.

LC-MS/MS and bioinformatics analysis

Approximately 1 μg of peptides were run on the pre-column (Acclaim PepMap™ 100, 75μm × 2cm, nanoViper, Thermo Scientific) and the analytical column (Acclaim PepMap™ RSCL, 75 μm × 50 cm, nanoViper, Thermo Scientific). The peptides were eluted using a 125-min linear gradient of ACN (9–45 %) in 0.1% FA and introduced to the mass spectrometer with a nanospray source. The parameters for the method were set as follows: nanospray needle voltage in positive mode: 1950 V; column flow rate: 0.300 μl/min; loading pump flow: 4 μl/min; inject mode: μl PickUp; Orbitrap MS scan resolution 120.000; scan range 197–1500 m/z; Orbitrap MS2 scan resolution: 15.000.

All collected spectra were searched against the Swiss-Prot database (selected for Homo sapiens, 2019_06, 20432 entries) on MASCOT (vs. 2.6.2). The parameters on MASCOT were set as follows: enzyme: trypsin, max missed cleavage: 2, peptide charge: 1+, 2+ and 3+, peptide tolerance: ± 0.6 Da, fixed modifications: carbamidomethyl (C), variable modifications: oxidation (M). Scaffold (vs. 4.8.7) was used to validate MS/MS-based peptide and protein identifications. The parameters on Scaffold were set as follows: protein threshold: 99%, peptide threshold: 90%, minimum number of peptides identified: 2.

Immunohistochemistry

Tumor sections from KPC and KPCC were obtained from different stages of PC progression. All slides were kept at 58°C overnight. The following day, the slides were cooled to room temperature and washed (4 × 10 min) using 100% xylene to remove paraffin. Subsequently, the slides were hydrated through alcohol solution (100%, 90%, 80%, 50%, 30%, and 20%) for 10 min each. The slides were then quenched of peroxidase activity through incubation with H_2O_2 in methanol (3%) for 1 hour in the dark. Antigen retrieval was further performed by incubating tissue slides with a 0.01M citrate buffer (pH 6.8). Tissue sections were blocked with either 2.5% horse serum or 3% bovine serum albumin (BSA) for 1 hr. Next, primary antibody (CST CD44, 1:500) or biotinylated *vicia villosa* (VVA) lectin (Vector Labs, 2.5 μg/mL) was added to tissue slides and incubated overnight at 4°C. The next day, the slides were washed in PBS-T (3 × 10 min) and PBS (1 × 10min), slides were probed with HRP-labelled universal anti-mouse/rabbit IgG or streptavidin-HRP (VectorLabs, 2μg/mL) for 1 hr. The slides were then stained with a DAB substrate kit (VectorLabs) and counterstained with hematoxylin, dehydrated using increasing alcohol concentrations, xylene washes, and mounted with Permount mounting medium (Fisher Scientific, Grand Island, NY, USA). Pathological scoring was performed by a pathologist using intensity score (0 weak to 3-intense staining) and percentage of cells given as a scale from 1–4 (1:0–24%, 2:25–49%, 50–74%, and 75–100%).

Immunofluorescence

For fluorescent analysis of CSC markers and Tn-antigen presentation, cells were seeded at 80% confluency on coverslips. Following washing with Hanks-buffer saline solution (HBSS), cells were fixed at −20°C with pre-chilled methanol for 5 minutes. After fixation and three PBS washes, cells were blocked with 10% normal goat serum (NGS) or 4% bovine serum albumin (BSA). Following a minimum of one hour blocking, cells were incubated with primary antibodies overnight. Finally, cells were washed with PBS and

incubated with fluorophore-conjugated secondary antibody for 1 hour at room temperature in the dark. Staining for Tn-antigens was performed using conjugated VVA-Texas Red (EY Labs) for 45 minutes in conjunction with secondary antibody staining. Following mounting of cells with DAPI-medium (Vector, Burlingame, CA, USA), coverslips were applied, and the resulting immunofluorescence images were acquired using Zeiss LSM800 confocal microscope (Carl Zeiss Microimaging, Thornwood, NY). For fluorescence of human and mouse tissue sections, a similar procedure was used as previously mentioned [17].

Proximity Ligation Assay

Proximity ligation was performed using Duolink™ In Situ Red Starter Kit Mouse/ Rabbit (Cat#DUO92101, Sigma) according to the manufacturer's instructions. Briefly, human PDAC and adjacent normal pancreas tissue sections processed as described for immunofluorescence of tissue sections up to a point after antigen retrieval. Next, tissue sections were blocked with blocking solution in a humidified chamber for 1 hour at 37°C, and CD44 and Tn-antigen primary antibodies were diluted in antibody diluent. After overnight incubation, the tissue sections were washed with wash buffer A (3×5 min); diluted probes (1 : 5) were added for 1 hour at 37°C. Next, probes were then ligated with ligase for 1 hour at 37°C, and amplified for 100 minutes at 37°C. Finally, the samples were washed with wash buffer B (3×5min), and mounted with medium containing DAPI. Images were acquired by confocal microscope (LSM800).

Real-Time RT-PCR (qRT-PCR)

Total RNA was isolated and prepared from cells using Qiagen RNAeasy kit (Qiagen, Valencia, CA, USA) according to the manufacturer's instructions. cDNA synthesis reactions were performed using SuperScript Reverse Transcription reagents (Invitrogen). qPCR reactions were performed using 2 μl of cDNA, 10 μl of LighyCycler 480 SYBR Green I master mix (Roche, USA), and 5 μmol of each primer. mRNA expression and fold change values are reported following CT method. The expression of all genes was normalized to that of internal controls and expressed relative to the indicated reference sample. A list of gene specific primers is listed in Supplementary Table 2.

Flow Cytometric Analysis

Cell surface marker staining was performed by incubating 1×10^6 cells in PBS containing 2% BSA(bovine serum albumin) and stained with the following antibodies at 4°C for 30 minutes: CD44 PE (BD Biosciences), EpCAM PE-CF594 (BD Biosciences), and CD133 PerCP-eFluor 710 (eBiosciences). Cells were washed twice with PBS, counterstained with DAPI, and analyzed by flow cytometry.

Migration Assay

Migration assay was performed with a 24-transwell polycarbonate membrane insert (#3422, Corning) according to the manufacturer's instructions. Briefly, 2×10^4 cells suspended in serum-free media was added to the membrane insert, and serum-containing media was added to the well. After 36-h incubation, non-migratory cells were removed with a cotton swab, and migratory cells were fixed with 70% ethanol, stained with 1% crystal violet.

Migrated cells were counted, and the average number of cells per field was calculated. Metastatic sub-lines were previously generated using subsequent cultures in transwell Boyden-chambers [7].

Sphere Formation Assay

Tumor sphere formation assays using PC cells were performed as previously described [17]. Briefly, 5.0×10^4 cells human and syngeneic-derived tumor cells were plated in a 96-well ultra-low attachment plate and cultured in DMEM/F12 (Invitrogen, Grand Island, NY) medium supplemented with B27 (Invitrogen), epidermal growth factor (20 ng/mL, PeproTech, Rocky Hill, NJ), and fibroblast growth factor (10 ng/mL, PeproTech). Tumor spheres were analyzed and counted after ten days of culture using a phase-contrast microscope.

Side Population (SP) Analysis

Side population (SP) of putative CSCs were performed as previously described [18, 19]. Briefly, 1×10^6 cells/ml of human PC or syngeneic-derived cancer cells were washed with PBS, suspended in DMEM containing 10% FBS, and incubated with 2 μg/ ml of Hoescht 33342 (AnaSpec Inc., Fremont, CA, USA) fluorescent dye for 90 minutes at 37°C in the dark with intermittent shaking for 90 minutes at 37°C. Cells were incubated with 100 μM of Verapamil (Sigma, St Louis, MO, USA) for 20 minutes at 37°C with intermittent shaking prior to Hoescht 33342 staining. After incubation, cells were immediately washed thrice with cold PBS and resuspended for counterstaining with 1 mL of culture media containing 10 μg/ml of propidium iodide to label dead cells. After gating, SP and non-SP cells were analyzed using BD LSR II Green flow cytometer (BD Biosciences, San Jose, CA).

In vivo limiting dilution assay

Cell suspension of KPC and KPCC cells were counted and resuspended in 60μl PBS at varying dilutions (1.0×10^5, 5.0×10^4, 1.0×10^4, and 1.0×10^3) and mixed with Matrigel (Becton Dickson, Franklin Lakes, NJ) in a 1:1 ratio. Next, cells in a 12μl PBS-Matrigel mix were injected subcutaneously into the left and right flanks of 7- to 8-week-old athymic nude mice. A total of three flanks were used for each group, and the appearance of tumors was assessed by palpitation two times per week and used to calculate tumor volume (mm^3) using the formula length x width$^2 \times 0.5$.

In vivo tumorigenesis and metastasis

Orthotopic implantation assays were performed as previously described [20]. Briefly, cells were infected with purified mCherry/Luciferase viral particles (GeneCopoeia, MD, USA) and maintained in puromycin-containing media followed by FACS sorting. A total of 0.25×10^6 cells in 50 μl of PBS were injected orthotopically into athymic nude mice (n=9) under aseptic conditions in the presence of ketamine/xylazine anesthesia. Organs and tumors were harvested 4 weeks following injections. Tumor growth was monitored by bioluminescence *in vivo* imaging systems (IVIS) after injection of 100μl of D-luciferein (15mg/ml) intraperitoneally.

Results

C1GALT1 deficient PC models identified aberrant O-glycosylation on CD44

To identify glycoproteins harboring aberrant O-glycosylation that could mediate the effects in aggressive PC, proteomic analyses of Tn-antigen glycoproteins were performed using control and CRISPR/Cas9 KO of C1GALT1 in PC cell lines. Lectin-affinity enrichment using *Vicia Villosa* (VVA) lectin was completed and subsequently used to identify Tn-antigen-containing glycoproteins using LC-MS/MS (Fig. 1A). The mass spectrometric analysis identified several hundred proteins in control and C1GALT1 KO T3M4 cells. Interestingly, CD44 was determined to be the most statistically significant and differentially glycosylated protein harboring Tn-antigens in C1GALT1 KO PC cells (Fig. 1B, Supplementary Table 3). Previous reports support Tn-antigen modification on CD44, where analytical glycoproteomic analyses identified Tn-antigens on CD44 in human O-GalNAc proteome using SimpleCell technology [21]. Consistently, our *in-silico* analysis using Net-O-Glyc 4.0 revealed several putative O-glycosylation sites present on the extracellular domain of CD44 (Supplementary Table 4). Among the identified proteins identified by MS, the significant and differentially expressed proteins in C1GALT1 KO T3M4 cells were used to perform DAVID gene ontology enrichment analysis. The analysis revealed an enrichment in categories comprised of cellular, biological, and mechanistic functions associated with Tn-antigen truncation, such as cell-cell interactions, adhesions, protein binding, and NF-κB signaling with enrichment scores (orange lines) above 1.5 (Fig. 1C). Further, enrichment with VVA lectin was performed in multiple cell lines to assess the abundance of CD44 containing Tn-antigens. In accordance with our proteomic analysis, loss of C1GALT1 in human PC cell lines and syngeneic-derived cell lines showed enrichment of Tn-antigens on CD44 compared to their respective controls (Fig. 1D). We next assessed CD44 and Tn-antigen staining at the aggressive 20-week stage of PC in the presence and absence of C1GALT1 using animal models of KrasG12D/+; Trp53R172H/+; Pdx-1-Cre (KPC) and KrasG12D/+; Trp53R172H/+; C1galt1loxP/loxP;Pdx-1-Cre (KPCC), respectively. We observed an increase in high-intensity staining of CD44 and Tn-antigen (using VVA lectin) observed in primary tumor xenografts from KPCC-derived animals compared to KPC (Fig. 1E). We observed that a similar increase in intensity staining in CD44 and Tn-antigen accumulation in ductal cells as early as 5 weeks to the 15-week stage of KPCC compared to KPC (Supplementary Fig. 1A). To determine whether side-specificities of VVA lectin is attributing to Tn-antigen staining, we employed LacdiNAc (GalNAcβ$_1$-$_4$GlcNAc)-specific antibody. We did not observe any drastic differences between T3M4 control compared to C1GALT1 KO cells or syngeneic-derived tumor cells, KPC or KPCC (Supplementary Fig. 1B). We further corroborated our previous findings of Tn-antigen present on CD44 by proximity ligation assay (PLA), where we found increased levels of Tn-antigens and CD44 in human PDAC tissue samples compared to the adjacent normal pancreas (Fig. 1F). Additionally, we did observe co-localization of CD44 and Tn-antigen in human PDAC tissue samples compared to the adjacent normal pancreas (Supplementary Fig. 1C). However, we did not observe considerable expression of LacdiNAc in human PDAC tissue samples (Supplementary Fig. 1D). Although several reports consistently attribute the glycosylation of proteins to have a wide array of effects on cancer [22, 23], none have directly contextualized its significance to a particular protein.

These results identify CD44 as a candidate glycoprotein harboring Tn-antigen structures in PC.

Truncation of O-glycosylation enhances CSCs features

The effects of O-glycosylation truncation were investigated to determine its impact on molecular regulators that drive gene expression and the functional features of CSCs since CD44 was identified as the top differentially glycosylated protein-containing Tn-antigens in C1GALT1 KO T3M4 cells. We observed an increased expression of several CSC markers of self-renewal and maintenance, such as NANOG, KLF4, and SOX9, in C1GALT1 KO cells, whereas a minimal difference was observed in CD133 (Fig. 2A). Additionally, increased expression of ABC transporter family members ABCG2 was observed, which has been shown to have an essential role in excluding cell-soluble molecules, a functional feature of CSCs [24]. Additionally, we also observed a significant increase in nuclear expression of CSC markers, SOX9 and KLF4, that coincides with CD44 membrane expression in C1GALT1 KO compared to control PC cells (Fig. 2B). Next, mRNA expression of CSC markers was assessed using quantitative RT-PCR (qRT-PCR) analysis. An increase in CSC markers, KLF4, SOX9, OCT3/4, and NANOG, was observed in T3M4 C1GALT1 KO and syngeneic-derived tumor PC cells, compared to respective controls (Fig. 2C, 2D). Since transcription factors have a significant role in the self-renewal properties of CSCs, we assessed the expression of human stem cell transcription factors in PC cells using an RT-PCR[2] array (QIAGEN®). Among all the transcription factors, increased fold-change in NANOG expression was identified in C1GALT1 KO compared to control T3M4 cells (Fig. 2E, Supplementary Table 5). Next, we explored the formation of tumorspheres as it is a prominent feature of CSCs used to assess their ability to proliferate and grow in non-adherent conditions [17, 25]. Additionally, a trait to characterize putative CSCs is the ability of cells to efflux soluble molecules based on ABC transporters expression in cells, which is measured quantitatively using FACS-based *in vitro* analysis [18, 19]. A significant increase in tumorsphere formation was observed in C1GALT1 KO for human and syngeneic-derived tumor cells compared to control cells (Supplementary Fig. 2A, 2B). Additionally, a significant increase in the percentage of putative CSCs was observed in T3M4 C1GALT1 KO cells when measured by side-population (SP) analysis (Fig. 2F). Given that CSCs are capable of forming tumors at varying limiting dilutions, we investigated the capability of KPC and KPCC cells to initiate tumors in immunocompromised mice at varying cell concentrations. We observed that KPCC cells progressively increase tumor volume, size, and weight for each cell concentration used (Fig. 2G, 2H). These results reveal that Tn-antigen truncation undoubtedly influences cancer cell stemness and tumor initiation by enhancing CSC self-renewal and maintenance regulators.

Immature Tn-antigen truncation identified on CD44 in C1GALT1 KO PC cells

To further delineate O-glycan structures found on CD44, PC cells with and without C1GALT1 expression were utilized since it has been previously reported that CD44 harbors multiple O-GalNAc modification sites as measured by LC-MS/MS glycoproteomics [21]. We first investigated the expression of C1GALT1 and CD44 expression using The Cancer Genome Atlas (TCGA). We observed low C1GALT1 and high CD44 expression in tumor patient samples of PC (Supplementary Fig. 3A). In addition, we also identified decrease

(P=0.07) gene expression of normalized C1GALT1 TPM in aggressive tumor grades found using TCGA data analyses (Supplementary Fig. 3B). However, we observed a significant increase (P=0.0206) in CD44 expression with increased tumor grades (Supplementary Fig. 3C). We further investigated two prominent truncated O-glycan structures, Tn-antigen and Sialylated-Tn (STn), since it has been found to increase CSC features primarily implicated in gastrointestinal diseases [26–29]. Interestingly, Tn-antigens and Sialyl-Tn structures were increased using lectin blot analyses in C1GALT1 KO clones compared to T3M4 and HPAF/CD18 control cell lines (Supplementary Fig. 3D). We also confirmed decreased C1GALT1 expression found in KPCC compared to KPC control cells, as observed by immunofluorescence (Supplementary Fig. 3E). A decrease in molecular weight of CD44 was observed in human C1GALT1 KO clones and syngeneic-derived tumor cells, an indication of immature glycosylation (Fig. 3A, 3B). To assess truncated O-glycans present on CD44, we performed immunoprecipitation of CD44 followed by lectin blot analyses in C1GALT1 KO and T3M4 control cells. The Tn-antigen level found in CD44 precipitates using Tn-antigen recognition lectin, VVA, contained higher Tn-antigens in C1GALT1 KO clones compared to control T3M4 cells (Fig. 3C). Additionally, the presence of Sialyl-Tn structures on CD44 was investigated using immunoprecipitates from PC cells. However, no differences were observed in sialylated oligosaccharides present on CD44 in C1GALT1 KO compared to control T3M4 cells (Supplementary Fig. 3F). Next, we assessed Sialylated oligosaccharides (Sialyl-Tn) using the sialic acid recognition lectin, SNA. However, no significant differences were observed between C1GALT1 KO and control T3M4 cells (Fig. 3D). Additionally, we employed Sialyl-Tn specific antibody and observed no drastic difference in the levels of STn- present on CD44 in control and T3M4 C1GALT1 KO cells (Supplementary Fig. 3G). Lastly, we sought to identify whether CD44 and Tn-antigens co-colocalize at the cell membrane using. An increase in membrane co-localization of CD44 and Tn-antigens were observed in C1GALT1 KO, whereas minimal co-localization in was observed in control T3M4 and KPC control cells (Fig. 3E). Line intensity plot scans highlight the co-localization at the cell membrane shown to the right of the merged image represented in the top right corner box (white dashed lines). Overall, these results support that CD44 is a highly O-glycosylated protein consisting of Tn-antigens resulting from C1GALT1 KO.

Truncation of CD44 glycosylation promotes CSCs through NF-κB signaling

Indeed, reports have emerged that propose loss of C1GALT1 enhances features and self-renewal properties of CSCs [30]. However, the effects of Tn-antigen truncation of glycoproteins on CSCs and the impact of stemness in aggressive cancer metastasis remain largely unexplored. We evaluated the mechanistic underpinnings of CD44 O-linked glycosylation to activate CSC self-renewal and maintenance. An additional sgRNA transfection was performed to generate CRISPR/Cas9 double knockouts of CD44 and C1GALT1, thus understanding the effect of Tn-antigen truncation of CD44. Using western blot analyses, a loss of CD44 in existing T3M4 C1GALT1 KO cells resulted in decreased NANOG protein expression and minimal variation in other CSC markers, including SOX2, KLF4, OCT3/4, MDR1, and β-catenin (Fig. 4A). Consistently, a loss of CD44 in T3M4 C1GALT1 KO cells affected CSC markers showing a reduction in mRNA expression for NANOG and other CSC and self-renewal markers, KLF4, OCT3/4, and ABCG2

(Supplementary Fig. 4A). The stemness-related marker, NANOG, was primarily affected by a loss of CD44 in existing T3M4 C1GALT1 KO cells. To determine the underlying effects of metastasis in PC animal models with C1GALT1 KO [7], we assessed several putative CSC signaling pathways that have been previously shown to alter CSC marker expression [14, 31]. An increase in phosphorylated signaling pathways ERK and NF-κB were found to increase in T3M4 C1GALT1 KO cells, whereas a decrease in both was found in C1GALT1 and CD44 double KO (Fig. 4B). However, a loss of CD44 in T3M4 PC cells did not alter the protein expression of stemness-related markers (SOX9, NANOG) or NF-κB (Supplementary Fig. 4B). Next, we characterized the population of putative cancer stem cells using SP analysis, which was decreased in C1GALT1 and CD44 double KO compared to T3M4 C1GALT1 KO cells (Fig. 4C). However, a loss of T3M4 CD44 KO cells did not significantly alter the SP population compared to control cells (Supplementary Fig. 4C). A loss of CD44 and C1GALT1 was also found to decrease the ALDH cell population compared to T3M4 C1GALT1 KO cells (Supplementary Fig. 4D). Similarly, a significant reduction in cells capable of forming tumorspheres was observed in C1GALT1 and CD44 double KO cells compared to T3M4 C1GALT1 KO cells (Fig. 4D). Specific CSC markers have been used to identify pancreatic CSCs, such as CD133, CD44, and EpCAM [32]. A significant decrease in the percentage of multi-stained markers of CSC cells, EpCAM$^+$/CD133$^+$/CD44$^+$, was observed in C1GALT1 & CD44 double KO PC cells compared to T3M4 C1GALT1 KO cells (Fig. 4E). Interestingly, Tn-antigen truncation on CD44 was found to co-localize with NANOG in T3M4 C1GALT1 KO compared to C1GALT1 & CD44 double KO cells (Fig. 4F). Additionally, CD44 and Tn-antigen co-localized at the cell membrane and higher nuclear staining of NANOG in T3M4 C1GALT1 KO PC cells compared to C1GALT1 and CD44 double KO cells as measured by line intensity plot scans. In addition, a significant increase in nuclear staining for NANOG was observed in T3M4 C1GALT1 KO cells compared to C1GALT1 & CD44 double KO cells. These results indicate that the Tn-antigen truncation of CD44 glycosylation enhances the expression of self-renewal genes and features of pancreatic CSCs.

Tn-antigen truncation of CD44 enhances stemness and NANOG expression through NF-kB signaling in syngeneic-derived tumor cells

To determine the significance of Tn-antigen truncation of CD44 to facilitate and aggravate PC, we employed engineered models of PC with and without C1GALT1 expression using KPC and KPCC, respectively. We developed KPC and KPCC cells with stable-knockdown of CD44 and observed a reduction in phosphorylated NF-κB in CD44 shRNA KPCC cells compared to shRNA KPCC shRNA control cells (Fig. 5A). However, a minimal variation of phosphorylated NF-κB was observed in CD44 knockdown KPC cells and shRNA control KPC cells. Additionally, a knockdown of CD44 in KPCC cells decreased protein expression in CSC markers, SOX9, KLF4, MDR1, and NANOG compared to control KPCC shRNA control cells. We also observed a significant reduction in *Nanog*, *Sox2*, and *Sox9* in KPCC and KPC CD44 knockdown cells compared to shRNA control cells (Fig. 5B, 5C). However, a more significant reduction of self-renewal and maintenance markers was observed in KPCC than KPC cells transfected with CD44 shRNA. Immunofluorescence analysis was performed using xenograft tissues from spontaneous tumor models of KPC and KPCC to determine the effects of Tn-antigen truncation and CD44 on other CSC markers. An

increased expression for CSC markers, SOX9 and DCLK1, and MDR1 and DCLK1, was observed using immunofluorescence in 20-week KPCC primary tumor tissues compared to 20-week KPC controls (Supplementary Fig. 5A and 5B). We next found Tn-antigen truncation on CD44 co-localizing with SOX9 at an aggressive 20-week stage in KPCC primary tumor tissues compared to KPC control (Fig. 5D). Since we had observed a decrease in NF-kB and NANOG expression in PC cells with CD44 and C1GALT1 double KO, we sought to identify the involvement of NF-kB regulation. The effects of NF-kB inhibition were assessed using inhibitor Dimethylaminoparthenolide (DMAPT), which acts to prevent the nuclear binding of phosphorylated NF-kB, p-65. We utilized the T3M4 C1GALT1 KO and KPCC cell lines treated with 2 μM of DMAPT, which inhibited cell viability to 50% (Supplementary Fig. 5C and 5D). A reduction of NANOG expression was shown in C1GALT1 KO human PC and KPCC cells due to NF-kB inhibition (Fig. 5E & 5F). These results suggest that Tn-antigens on CD44 enhances CSC features through increased expression of NANOG via NF-κB signaling. (Fig. 5G)

O-glycosylation truncation of CD44 modulates tumorigenesis and metastasis

To examine the effects of Tn-antigen truncation of CD44 on tumor growth, both *in vitro* and *in vivo* approaches were performed using T3M4 PC cells. A significant increase in migratory potential was observed in T3M4 C1GALT1 KO compared to control cells (Supplementary Fig. 6A). However, a loss of CD44 in the existing T3M4 C1GALT1 KO significantly decreased the migration potential. Similarly, a significant increase in colony formation was observed in T3M4 C1GALT1 KO compared to control cells, where a similar reduction was rescued in C1GALT1 and CD44 double KO cells (Supplementary Fig. 6B). We next performed *in vivo* orthotopic injection experiments using T3M4 control, C1GALT1 KO, and C1GALT1 and CD44 double KO cells carrying a luciferase reporter gene to understand the effect of tumor growth modulation by Tn-antigen truncation on CD44. After four weeks post-injection, mice were euthanized and dissected for primary tumor and organ collection. A loss of C1GALT1 significantly augmented tumor weights compared to T3M4 control cells; however, C1GALT1 and CD44 double KO significantly reduced tumor weight (Fig. 6A). In addition, a significant increase in average radiance occurred after several weeks at the site of the pancreas in animals injected with C1GALT1 KO cells compared to control T3M4 cells. However, C1GALT1 and CD44 double KO cells showed minimal average radiance readings due to tumor size being less than 1cm (Supplementary Fig. 6C). Interestingly, a loss of CD44 in T3M4 PC cells was did not impact the reduction of *in vivo* tumor weight compared to C1GALT1 and CD44 double KO (Supplementary Fig. 6D). We next determined the co-localization of CD44 and Tn-antigen as it pertains to NANOG expression by using primary tumors sections from the orthotopic implantation experiment. Indeed, we observed increased membrane co-localization of CD44-containing Tn-antigen truncation coinciding with increased NANOG expression in animals injected with T3M4 C1GALT1 KO (Fig. 6B). Using histology H&E staining from the liver (Fig. 6C) and lungs (Fig. 6D), a significant increase in micrometastases was observed in animals injected with T3M4 C1GALT1 KO cells compared to control cells and C1GALT1 and CD44 double KO cells, which coincides with IVIS ex-vivo imaging from these organs. We next utilized migratory T3M4 sublines developed using serial Boyden-chambers from low to highly migratory cells (M1 to M4) compared to parental cells. We observed increased

protein expression of CD44 and NANOG in increasing migratory sublines parental T3M4 cells (Fig. 6E). Additionally, we observed a similar increase from bioluminescence using ex-vivo imaging from additional organs, such as the diaphragm, lymph node, and peritoneum (Supplementary Fig. 6E). Similarly, organs collected from the lung and liver contained Tn-antigen, CD44, and NANOG co-localization from animals injected with T3M4 C1GALT1 KO cells, which was not observed in control, and C1GALT1 and CD44 double KO cells (Fig. 7A and 7B). These results indicate that the O-glycosylation truncation of CD44 drives tumorigenesis and stemness properties of pancreatic CSCs.

Discussion

The core-1 galactosyltransferase enzyme or C1GALT1 is an enzyme that transfers a single galactose monosaccharide onto the existing GalNAc-Ser/Thr found on many proteins. The effect of aberrant O-GalNAc modification on glycoproteins has been shown to influence oncogenic and aggressive features of PC [7, 10, 30, 33, 34]. Several transmembrane proteins, including mucins, EGFR, HER2, and CD44, are instrumental in promoting proliferation, metastasis, and cancer stem-like phenotypes [8, 27, 35]. The effect of glycoproteins in cancer cells is attributed to the status of O-linked glycosylation. Gilad et al. have shown that linear polysaccharide hyaluronan on CD44 mediates activation of the NANOG transcription factor for maintenance and self-renewal of cells in breast and ovarian tumor cells [36]. Similarly, recent studies have shown that inhibition of the signaling pathway NF-kB disrupts CSC maintenance and stemness genes (e.g., SOX, OCT4, NANOG, KLF4) [37, 38]. Although much has been shown on the effect of aberrant O-glycosylation in cancer cells, few reports exist that illustrate the significance of specific glycoproteins and their downstream impact on CSCs and metastasis.

GalNAc-transferase enzymes initiate the process of O-GalNAc modification (e.g., GALNT's) that can modify various cell surfaces and secreted proteins. Recent studies have shown that immature O-linked glycosylation largely correlates with aggressiveness of PC, mainly due to overactive GALNT's or C1GALT1 and COSMC inactivation [7, 10, 39]. Our study identified that aberrant Tn-antigen modification, mediated by a loss of C1GALT1, is essential for aggressive metastatic properties and enrichment of pancreatic CSCs. A lectin-based glycoprotein enrichment approach identified CD44 as a top differentially glycosylated protein as a result of C1GALT1 KO in PC cells, a pattern similarly observed in increased tumor grades of PC. Interestingly, we identified NANOG to be elevated and was found to be the most differentially expressed amongst several putative CSC transcription factors in C1GALT1 KO PC cells. We also identified the upregulation of stemness and CSC features in human PC and syngeneic-derived tumor cells with C1GALT1 KO. Our study shows that in PC, loss of C1GALT1 results in aberrant Tn-antigen accumulation present on CD44, a glycoprotein with several putative O-glycosylation sites. To further support the modification of Tn-antigens on CD44, we performed lectin-enrichment assays and cellular co-localization analysis to identify CD44 to be a heavily O-glycosylated protein that overlaps with Tn-antigen truncation at the cell membrane.

A prominent signaling pathway known to be upregulated in PC is the NF-kB cellular signaling pathway, promoting tumor growth and resistance of PC. Activation of NF-kB

has also been identified as one of the mechanisms that mediate the self-renewal of CSCs [40]. Previously, others have determined that hyaluronan-dependent activation of CD44 is required for downstream activation of NF-kB that results in the expression of MDR1 in breast cancer cells [36]. However, CD44 contains several putative O-glycosylation sites that undergo immature O-glycosylation truncation because of a loss of C1GALT1 in PC. Our study identified a decrease in expression of stemness-related genes, CSC features, and populations of putative CSCs (e.g., CD44^{+}/EpCAM^{+}/CD133^{+}) in C1GALT1 and CD44 double KO cells. We propose that the immature O-glycosylation of CD44 allows for malignant transformation and enriches the CSC population through NANOG activation via NF-kB. Firstly, we identified a considerable decrease in NF-kB phosphorylated p65 subunit in C1GALT1 and CD44 double KO cells. To determine the regulation of NANOG activity by NF-kB, we implemented DMAPT, an allosteric inhibitor of cysteine on phosphorylated NF-kB (p65), which prevents nuclear translocation and DNA binding [41]. Using DMAPT resulted in a reduction of phosphorylated NF-kB and NANOG expression in PC and syngeneic-derived tumor cells with C1GALT1 KO. Our results begin to provide insight on aberrant O-glycosylation and indicate a substantial contribution of NF-kB signaling to the cancer stem-like phenotype in PC.

In addition to NANOG, several CSC markers (KLF4, SOX9, OCT3/4) and drug-resistance markers (MDR1 and ABCG2) were overexpressed in C1GALT1 KO PC cells, which highlights the impact of CSC enrichment. NANOG has been characterized as a transcription factor known to regulate key molecules for stemness markers [42], possibly through the cooperation of the genes mentioned above to maintain stemness in PC cells. Additionally, we found that a concomitant loss of CD44 expression in C1GALT1 KO cells hindered any growth advantage driven by aberrant Tn-antigen truncation pertaining to tumor growth, migration, and metastases. Our data begins to highlight aberrant O-glycosylation of CD44 as a target for inhibiting cancer stem-like cells and the inherent metastatic properties that underlie PC aggressiveness and enriched stemness features (Fig. 7C).

Currently, PC is one of the harshest malignancies with limited treatment options. Surgical resection, sudden relapse after chemotherapies, and compounded metastases are common occurrences. Therefore, the development of innovative therapeutics and new target discoveries are essential in PC. Our study highlights the therapeutic potential of CD44 containing several putative O-glycosylation sites and is commonly overexpressed in aggressive cancers. Our work provides a rationale for the future design of small-molecule inhibitors against CD44 containing aberrant post-translational modifications to prevent and treat established metastasis and cancer stem cells.

Supplementary Material

Refer to Web version on PubMed Central for supplementary material.

Acknowledgements

References

1. Alison MR, Lim SML, Nicholson LJ. Cancer stem cells: problems for therapy? Journal of Pathology 2011; 223: 147–161.

2. Nimmakayala RK, Batra SK, Ponnusamy MP. Unraveling the journey of cancer stem cells from origin to metastasis. Biochimica et Biophysica Acta (BBA) - Reviews on Cancer 2019; 1871: 50–63. [PubMed: 30419314]

3. Kreso A, Dick John E. Evolution of the Cancer Stem Cell Model. Cell Stem Cell 2014; 14: 275–291. [PubMed: 24607403]

4. Li C, Heidt DG, Dalerba P, Burant CF, Zhang L, Adsay V et al. Identification of pancreatic cancer stem cells. Cancer Research 2007; 67: 1030–1037. [PubMed: 17283135]

5. Fang R, Xu F, Shi H, Wu Y, Cao C, Li H et al. LAMTOR5 raises abnormal initiation of O-glycosylation in breast cancer metastasis via modulating GALNT1 activity. Oncogene 2019; 39: 2290–2304. [PubMed: 31836847]

6. Scott E, Munkley J. Glycans as Biomarkers in Prostate Cancer. Int J Mol Sci 2019; 20: 1389.

7. Chugh S, Barkeer S, Rachagani S, Nimmakayala RK, Perumal N, Pothuraju R et al. Disruption of C1galt1 Gene Promotes Development and Metastasis of Pancreatic Adenocarcinomas in Mice. Gastroenterology 2018; 155: 1608–1624. [PubMed: 30086262]

8. Chugh S, Meza J, Sheinin YM, Ponnusamy MP, Batra SK. Loss of N-acetylgalactosaminyltransferase 3 in poorly differentiated pancreatic cancer: augmented aggressiveness and aberrant ErbB family glycosylation. British Journal Of Cancer 2016; 114: 1376–1386. [PubMed: 27187683]

9. Gupta R, Leon F, Thompson CM, Nimmakayala R, Karmakar S, Nallasamy P et al. Global analysis of human glycosyltransferases reveals novel targets for pancreatic cancer pathogenesis. British Journal of Cancer 2020; 122: 1661–1672. [PubMed: 32203219]

10. Radhakrishnan P, Dabelsteen S, Madsen FB, Francavilla C, Kopp KL, Steentoft C et al. Immature truncated O-glycophenotype of cancer directly induces oncogenic features. Proceedings of the National Academy of Sciences 2014; 111: E4066–E4075.

11. Beça FFd, Caetano P, Gerhard R, Alvarenga CA, Gomes M, Paredes J et al. Cancer stem cells markers CD44, CD24 and ALDH1 in breast cancer special histological types. Journal of Clinical Pathology 2013; 66: 187–191. [PubMed: 23112116]

12. Li W, Ma H, Zhang J, Zhu L, Wang C, Yang Y. Unraveling the roles of CD44/CD24 and ALDH1 as cancer stem cell markers in tumorigenesis and metastasis. Scientific Reports 2017; 7: 13856. [PubMed: 29062075]

13. Wang L, Zuo X, Xie K, Wei D. The Role of CD44 and Cancer Stem Cells. In: Papaccio G, Desiderio V (eds). Cancer Stem Cells: Methods and Protocols. Springer New York: New York, NY, 2018, pp 31–42.

14. Barkeer S, Chugh S, Batra SK, Ponnusamy MP. Glycosylation of Cancer Stem Cells: Function in Stemness, Tumorigenesis, and Metastasis. Neoplasia 2018; 20: 813–825. [PubMed: 30015157]

15. Chia J, Goh G, Bard F. Short O-GalNAc glycans: regulation and role in tumor development and clinical perspectives. Biochimica et Biophysica Acta (BBA) - General Subjects 2016; 1860: 1623–1639. [PubMed: 26968459]

16. Sanjana NE, Shalem O, Zhang F. Improved vectors and genome-wide libraries for CRISPR screening. Nature Methods 2014; 11: 783–784. [PubMed: 25075903]

17. Nimmakayala RK, Seshacharyulu P, Lakshmanan I, Rachagani S, Chugh S, Karmakar S et al. Cigarette Smoke Induces Stem Cell Features of Pancreatic Cancer Cells via PAF1. Gastroenterology 2018; 155: 892–908.e896. [PubMed: 29864419]

18. Goodell MA, Brose K, Paradis G, Conner AS, Mulligan RC. Isolation and functional properties of murine hematopoietic stem cells that are replicating in vivo. The Journal of Experimental Medicine 1996; 183: 1797–1806. [PubMed: 8666936]

19. Vaz AP, Ponnusamy MP, Rachagani S, Dey P, Ganti AK, Batra SK. Novel role of pancreatic differentiation 2 in facilitating self-renewal and drug resistance of pancreatic cancer stem cells. British Journal Of Cancer 2014; 111: 486–196. [PubMed: 25003666]

20. Vaz AP, Deb S, Rachagani S, Dey P, Muniyan S, Lakshmanan I et al. Overexpression of PD2 leads to increased tumorigenicity and metastasis in pancreatic ductal adenocarcinoma. Oncotarget 2015; 7: 3317–3331.

21. Steentoft C, Vakhrushev SY, Joshi HJ, Kong Y, Vester-Christensen MB, Schjoldager KT-BG et al. Precision mapping of the human O-GalNAc glycoproteome through SimpleCell technology. The EMBO Journal 2013; 32: 1478–1488. [PubMed: 23584533]

22. Stowell SR, Ju T, Cummings RD. Protein glycosylation in cancer. Annu Rev Pathol 2015; 10: 473–510. [PubMed: 25621663]

23. Cummings RD. "Stuck on sugars – how carbohydrates regulate cell adhesion, recognition, and signaling". Glycoconjugate Journal 2019; 36: 241–257. [PubMed: 31267247]

24. Zhou S, Schuetz JD, Bunting KD, Colapietro A-M, Sampath J, Morris JJ et al. The ABC transporter Bcrp1/ABCG2 is expressed in a wide variety of stem cells and is a molecular determinant of the side-population phenotype. Nature Medicine 2001; 7: 1028–1034.

25. Abel EV, Simeone DM. Biology and Clinical Applications of Pancreatic Cancer Stem Cells. Gastroenterology 2013; 144: 1241–1248. [PubMed: 23622133]

26. Trinchera M, Aronica A, Dall'Olio F. Selectin Ligands Sialyl-Lewis a and Sialyl-Lewis x in Gastrointestinal Cancers. Biology 2017; 6: 16.

27. Remmers N, Anderson JM, Linde EM, DiMaio DJ, Lazenby AJ, Wandall HH et al. Aberrant Expression of Mucin Core Proteins and O-Linked Glycans Associated with Progression of Pancreatic Cancer. Clinical Cancer Research 2013; 19: 1981–1993. [PubMed: 23446997]

28. Dorsett KA, Jones RB, Ankenbauer KE, Hjelmeland AB, Bellis SL. Sox2 promotes expression of the ST6Gal-I glycosyltransferase in ovarian cancer cells. Journal of Ovarian Research 2019; 12: 93. [PubMed: 31610800]

29. Schultz MJ, Holdbrooks AT, Chakraborty A, Grizzle WE, Landen CN, Buchsbaum DJ et al. The Tumor-Associated Glycosyltransferase ST6Gal-I Regulates Stem Cell Transcription Factors and Confers a Cancer Stem Cell Phenotype. Cancer Research 2016; 76: 3978–3988. [PubMed: 27216178]

30. Freitas D, Campos D, Gomes J, Pinto F, Macedo JA, Matos R et al. O-glycans truncation modulates gastric cancer cell signaling and transcription leading to a more aggressive phenotype. EBioMedicine 2019; 40: 349–362. [PubMed: 30662000]

31. Rinkenbaugh AL, Baldwin AS. The NF-κB Pathway and Cancer Stem Cells. Cells 2016; 5: 16.

32. Lonardo E, Hermann Patrick C, Mueller M-T, Huber S, Balic A, Miranda-Lorenzo I et al. Nodal/Activin Signaling Drives Self-Renewal and Tumorigenicity of Pancreatic Cancer Stem Cells and Provides a Target for Combined Drug Therapy. Cell Stem Cell 2011; 9: 433–446. [PubMed: 22056140]

33. Thomas D, Sagar S, Caffrey T, Grandgenett PM, Radhakrishnan P. Truncated O-glycans promote epithelial-to-mesenchymal transition and stemness properties of pancreatic cancer cells. Journal of Cellular and Molecular Medicine 2019; 23: 6885–6896. [PubMed: 31389667]

34. Gill DJ, Tham KM, Chia J, Wang SC, Steentoft C, Clausen H et al. Initiation of GalNAc-type O-glycosylation in the endoplasmic reticulum promotes cancer cell invasiveness. Proceedings of the National Academy of Sciences 2013; 110: E3152–E3161.

35. Mimeault M, Batra SK. Molecular Biomarkers of Cancer Stem/Progenitor Cells Associated with Progression, Metastases, and Treatment Resistance of Aggressive Cancers. Cancer Epidemiology Biomarkers & Prevention 2014; 23: 234–254.

36. Bourguignon LYW, Peyrollier K, Xia W, Gilad E. Hyaluronan-CD44 interaction activates stem cell marker Nanog, Stat-3-mediated MDR1 gene expression, and ankyrin-regulated multidrug efflux in breast and ovarian tumor cells. J Biol Chem 2008; 283: 17635–17651. [PubMed: 18441325]

37. Kaltschmidt C, Banz-Jansen C, Benhidjeb T, Beshay M, Förster C, Greiner J et al. A Role for NF-κB in Organ Specific Cancer and Cancer Stem Cells. Cancers 2019; 11: 655.

38. Zakaria N, Mohd Yusoff N, Zakaria Z, Widera D, Yahaya BH. Inhibition of NF-κB Signaling Reduces the Stemness Characteristics of Lung Cancer Stem Cells. Frontiers in Oncology 2018; 8: 166. [PubMed: 29868483]

39. Ju T, Otto VI, Cummings RD. The Tn Antigen—Structural Simplicity and Biological Complexity. Angewandte Chemie International Edition 2011; 50: 1770–1791. [PubMed: 21259410]

40. Feitelson MA, Arzumanyan A, Kulathinal RJ, Blain SW, Holcombe RF, Mahajna J et al. Sustained proliferation in cancer: Mechanisms and novel therapeutic targets. Seminars in Cancer Biology 2015; 35: S25–S54. [PubMed: 25892662]

41. Ghantous A, Sinjab A, Herceg Z, Darwiche N. Parthenolide: from plant shoots to cancer roots. Drug Discovery Today 2013; 18: 894–905. [PubMed: 23688583]

42. Es-haghi M, Soltanian S, Dehghani H. Perspective: Cooperation of Nanog, NF-κB, and CXCR4 in a regulatory network for directed migration of cancer stem cells. Tumor Biology 2016; 37: 1559–1565. [PubMed: 26715265]
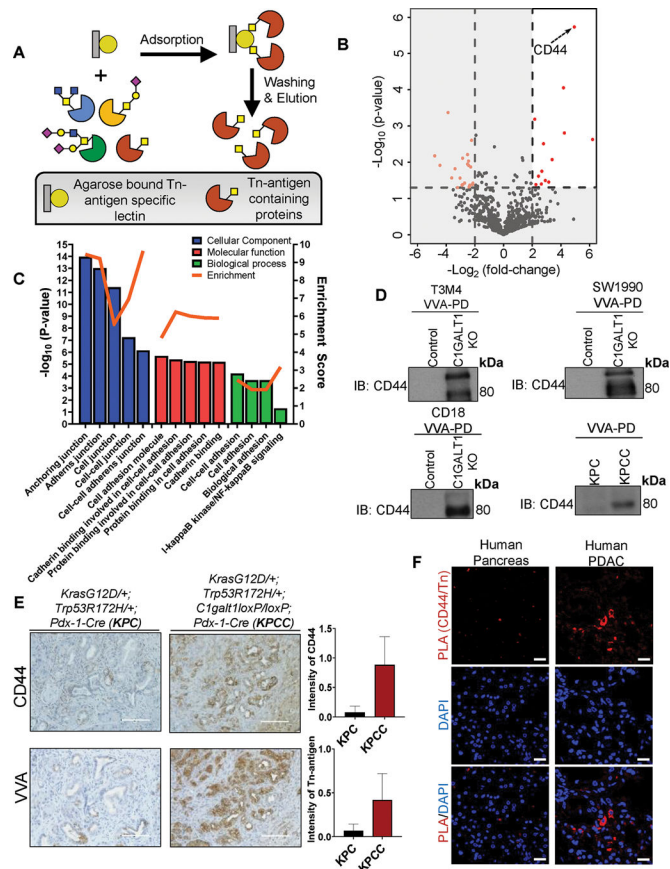
Figure 1. Mass spectrometry results identify CD44 as a marker of aberrant glycosylation in PC.
A) Schematic illustration of the experimental approach showing affinity enrichment of Tn-antigen glycoproteins by agarose bound *Vicia villosa* (VVA) lectin enrichment. B) Enriched Tn-antigen-containing proteins in T3M4 cells identified CD44 as a prominent glycoprotein in C1GALT1 KO cells. Volcano plot showing significant (red dots corresponding to identified proteins with a p-value <= 0.05) Tn-antigen enriched proteins. Positive $\log_2$ values indicate proteins enriched in C1GALT1 KO cells compared to control T3M4 cells (negative $\log_2$ values). C) Gene ontology term enrichment of significantly identified Tn-antigen proteins using DAVID bioinformatics resources 6.8. D) Whole-cell lysates from several PC cells were enriched for Tn-antigens using VVA. The subsequent precipitates were immunoblotted for CD44 in respective control and C1GALT1 KO PC cells. E) Immunohistochemical staining of CD44 and Tn-antigens (using VVA lectin) at aggressive 20-week stage KrasG12D/+; Trp53R172H/+; Pdx-1-Cre (KPC) and KrasG12D/+; Trp53R172H/+; C1galt1loxP/loxP;Pdx-1-Cre (KPCC) animal tumor sections are shown. The representative intensity score is shown to the right. Data are mean ± SD, *n*=3 F) Proximity ligation assay (PLA) showing interaction (red fluorochrome) between CD44 and Tn-antigen in human PDAC and adjacent normal pancreas tissue sections. Scale bar: 20μm. Significance was determined using Student's t-test. *P<0.05, **P<0.01, ***P<0.001, nonsignificant (n.s.), P> 0.05.
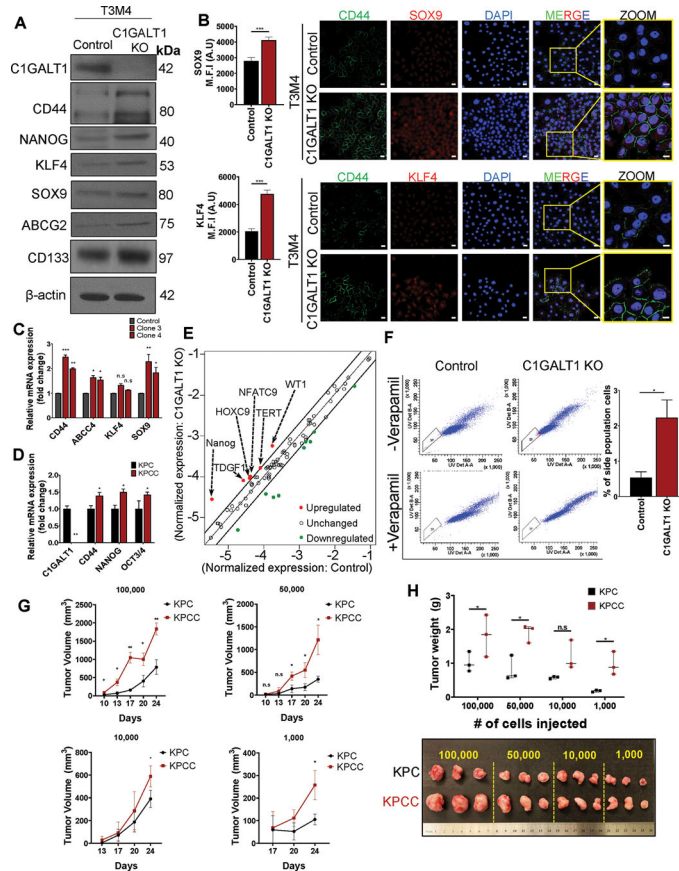
Figure 2. The loss of C1GALT1 enhances self-renewal markers and features of CSCs.
A) Immunoblot analysis of C1GALT1, CD44, CSC markers (ABCG2 and CD133), and self-renewal markers (NANOG, KLF4, SOX9) in T3M4 control and CRISPR/Cas9 C1GALT1 KO cells. B) Representative immunofluorescence images of CD44 and SOX9 in the cell membrane and nuclei, respectively, in T3M4 control and C1GALT1 KO cells. Similarly, CD44 and KLF4 immunofluorescence images are also shown. Quantification of the mean fluorescence intensity (M.F.I) is shown to the right. Data are mean ± SD, n=5. Scale bar: 20μm. C) Quantification of CSC and self-renewal marker mRNA expression in human T3M4 PC cells and D) xenograft-derived tumor cells (KPC and KPCC). Data are mean ± SD, n=3. E) RT^2 profiler PCR array (QIAGEN®) analysis of human transcription factors in T3M4 control and C1GALT1 KO cells. Upregulated genes are indicated in red, and genes significantly downregulated are indicated in green. F) Representative plots and quantification of the percentage of unique CSCs measured by FACS-based side population analysis in T3M4 control and C1GALT1 KO cells. Data are mean ± SD, n=3 G) Syngeneic-derived tumor cells, KPC and KPCC, were subcutaneously injected using limited dilutions in the left and right flanks of nude mice at varying cell number concentrations (1.0×10^5, 5.0×10^4, 1.0×10^4, and 1.0×10^3) and tumor volumes were measured for approximately three weeks. Data for each group are mean ± SD, n=3. H) Representative quantification of tumor weight and tumor images generated from subcutaneous experiments using KPC and KPCC syngeneic-derived tumor cells. Data are mean ± SD, n=3. Significance was

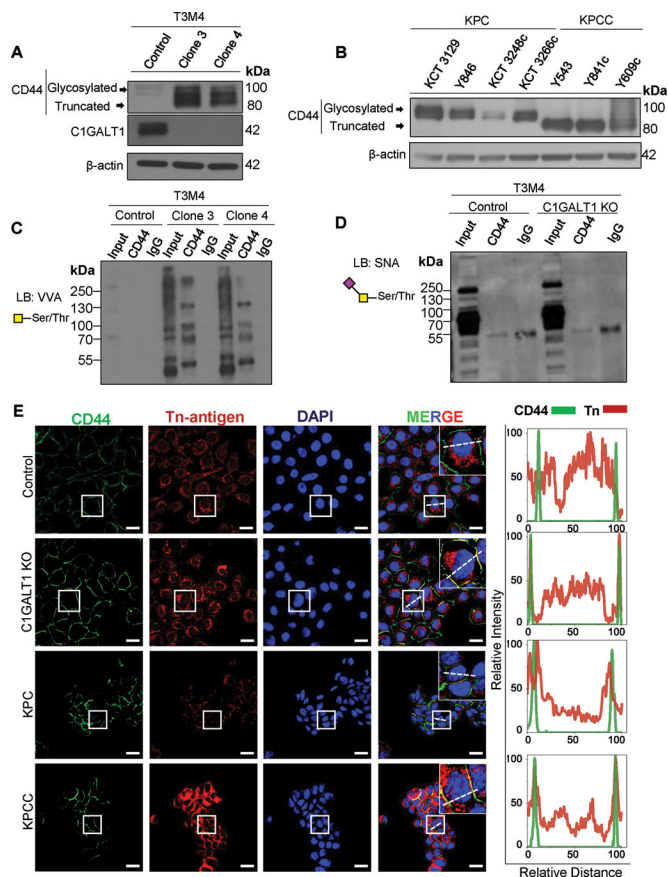determined using Student's t-test. *$P<0.05$, **$P<0.01$, ***$P<0.001$, nonsignificant (n.s.), $P > 0.05$.

Author Manuscript

Author Manuscript

Author Manuscript

Author Manuscript

Figure 3. CD44 is heavily o-linked with Tn-antigens in aberrant glycosylation of PC.
A) Immunoblot analysis of CD44 depicting glycosylated and O-linked truncation in T3M4 control and C1GALT1 KO cells. B) Several xenograft-derived tumor cell lines were developed and examined for CD44 containing glycosylated and O-linked truncation in control (KPC) and C1GALT1 KO cells (KPCC). C) Immunoprecipitation was performed with CD44 antibodies from T3M4 control and C1GALT1 KO cells, and subsequent lectin blot analysis was performed using VVA lectin. D) Immunoprecipitates of CD44 from T3M4 control and C1GALT1 KO cells were also used to perform lectin blot analysis of sialylated containing glycoproteins using SNA, *Sambucus niagra lectin*. E) Representative immunofluorescence images of CD44 and Tn-antigen structures in T3M4 control and C1GALT1 KO cells. Co-localization of CD44 and Tn-antigen is plotted in the line scans to the right of dashed lines shown in the highlighted boxes. Scale bar: 20μm.
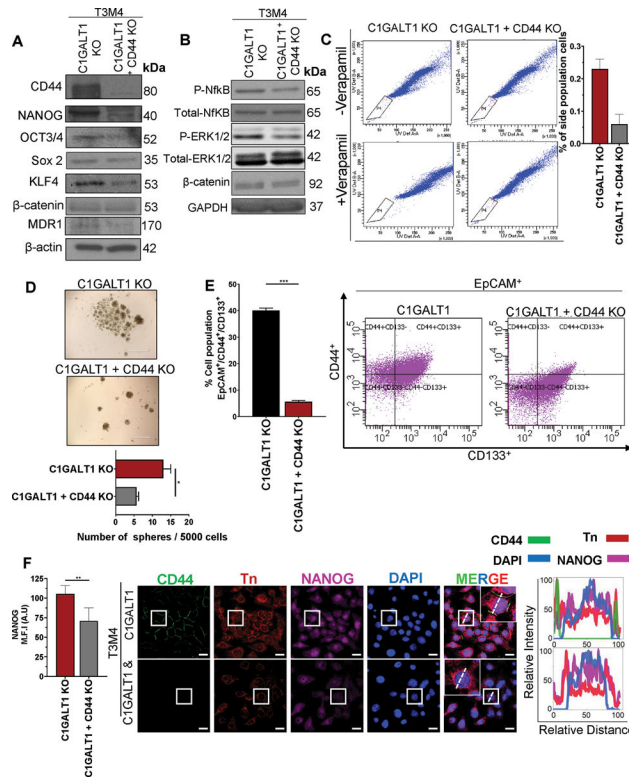
Figure 4. Truncation of Tn-antigen o-linked CD44 increases CSC features via NF-κB signaling.
A) Immunoblot analysis for CD44, NANOG, OCT3/4, SOX2, KLF4, β-catenin, and MDR1 in C1GALT1 KO alone and C1GALT1 + CD44 double KO T3M4 cells. B) Immunoblot analysis of signaling pathways NF-kB, IkK, ERK, and β-catenin in C1GALT1 KO and C1GALT1 + CD44 double KO T3M4 cells. C) Representative plots and quantification of the percentage of unique CSCs as measured by FACS-based side population analysis in C1GALT1 KO alone and C1GALT1 + CD44 double KO T3M4 cells. Data are mean ± SD, n=3. D) Representative images of tumorspheres in C1GALT1 KO alone and C1GALT1 + CD44 double KO T3M4 cells. Data are mean ± SD, n=3. E) Representative plots and quantification of cells stained for CD44^{+}, CD133^{+}, and EpCAM^{+} in C1GALT1 KO and C1GALT1 + CD44 double KO T3M4 cells. Data are mean ± SD, n=3. F) Representative immunofluorescence images of CD44, Tn-antigen, and NANOG in C1GALT1 KO and C1GALT1 + CD44 double KO T3M4 cells. Co-localization of CD44 and Tn-antigen are found in the cell periphery, and NANOG and DAPI are found in the nucleus, as demonstrated in the plotted line scans to the right of dashed lines shown in the highlighted boxes. Quantification of the mean fluorescence intensity (M.F.I) is shown to the right and presented as a mean of five individual cells. Scale bar: 20μm. Data are mean ± SD, n=3. Significance was determined using Student's t-test. $*P<0.05$, $**P<0.01$, $***P<0.001$.
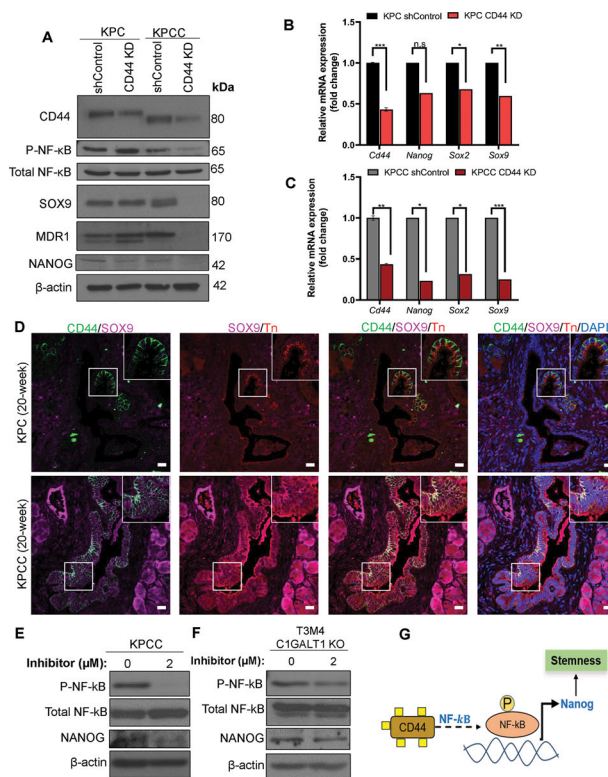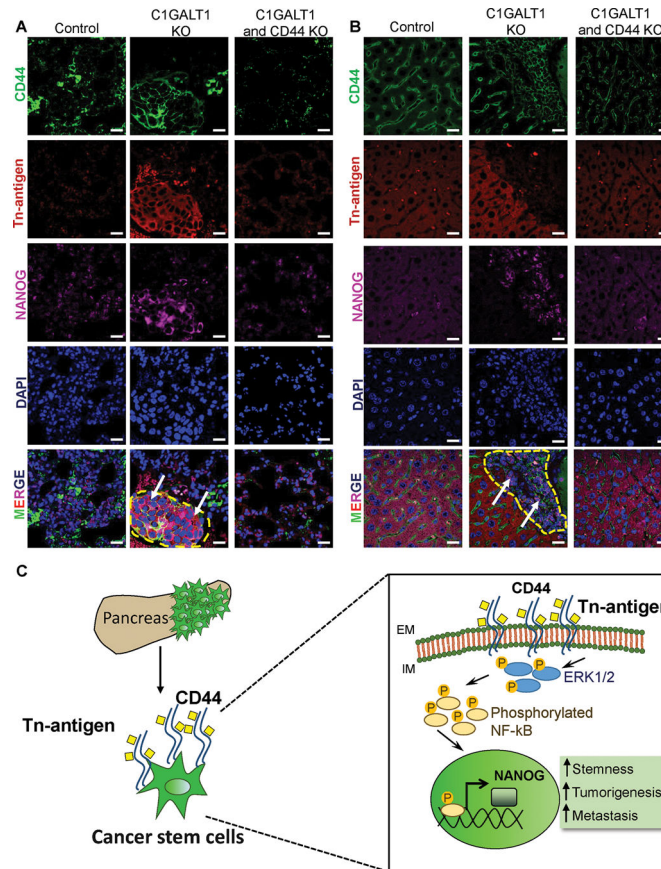
Figure 5. Tn-antigen truncation of CD44 elevates CSC features and NANOG expression via NF-kB signaling in PC cells.

A) Immunoblot analysis of CD44, activated and total NF-kB, SOX9, MDR1, and NANOG expression in xenograft-derived tumor cells of KPC and KPCC stably transfected with small-hairpin control (shControl) and small-hairpin CD44 (shRNA CD44 KD) constructs. B & C) Quantification of CD44 and CSC self-renewal marker (*Nanog, Sox2, and Sox9*) mRNA expression in KPC and KPCC cell lines. Data are mean ± SD, n=3. D) Representative immunofluorescence analysis of CD44, Tn-antigen, and SOX9 in KPC and KPCC syngeneic-derived tumor sections. Scale bar: 20μm. E) Immunoblot analysis for the activating subunit of NF-kB (p-65) and total NF-kB following 48-hour DMAPT treatment in KPCC xenograft-derived tumor cells and F) human C1GALT1 KO T3M4 cells. G) Schematic illustration of the proposed mechanism of O-linked Tn-antigens on CD44 facilitating downstream signaling of NF-kB for activation of NANOG to induce stemness properties of PC. Significance was determined using Student's t-test. *P<0.05, **P<0.01, ***P<0.001.
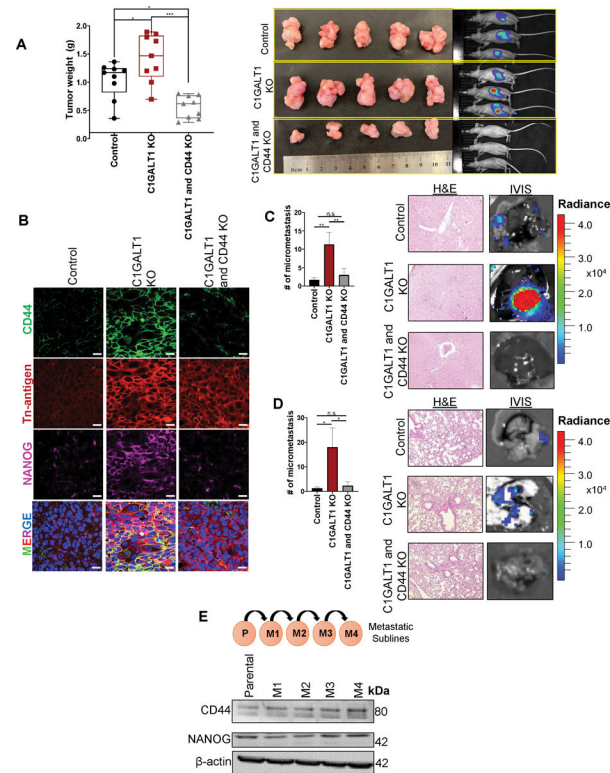
Figure 6. O-linked truncation of CD44 enhances *in vitro* and *in vivo* tumorigenesis.
A) Representative images and quantification of tumor weights from orthotopic implantation of control, C1GALT1 and C1GALT1 + CD44 double KO T3M4 cells in the pancreas of athymic nude/immunocompromised mice. Data are mean ± SD, n=9. B) Representative immunofluorescence analysis of CD44, Tn-antigens, and NANOG in animal tumor sections implanted with T3M4 control, C1GALT1 KO, and C1GALT1 + CD44 double KO cells. Scale bar: 20μm. C & D) Representative images and quantification number of micrometastases observed in the liver and lung, respectively, collected from orthotopic implantation experiments. Data are mean ± SD, n=3. IVIS images from the organs are also depicted adjacent to representative H&E images. E) Schematic representation of migratory sublines developed to assess protein expression in increasing migratory sublines (M1-M4) compared to parental T3M4 cells. Immunoblot analysis from PC sublines were assessed for CD44 and NANOG. Significance was determined using one-way ANOVA with the Tukey multiple comparison test. *P< 0.05; **, P< 0.005 and ***, P< 0.001.

Figure 7. O-glycan truncation of CD44 promotes metastasis of PC
A) Representative co-localization of CD44, Tn-antigen, and NANOG from the lung and
B) liver sections from orthotopic implantation experiments injected with T3M4 control,
C1GALT1 and C1GALT1 + CD44 double KO cells. Yellow highlighted region and white
arrows indicate areas of tumor cells. C) Representative illustration highlighting that a loss
of C1GALT1 expression promotes tumorigenesis and stemness properties in PC. Loss
of C1GALT1 in PC leads to O-glycan truncation on CD44 to activate the ERK/NF-κB
signaling. Consequently, this leads to enhanced NANOG expression to drive CSC self-
renewal properties and tumorigenesis observed in aggressive PC. Scale bar: 20μm.